



Exploring sesquiterpene lactone as a dual therapeutic agent for diabetes and oxidative stress: insights into PI3K/AKT modulation

Kadhirmathiyam Velumani¹ · Arun John² · Mohammed Rafi Shaik³ · Shaik Althaf Hussain⁴ · Ajay Guru⁵ · Praveen Kumar Issac¹

Received: 25 April 2024 / Accepted: 8 August 2024 / Published online: 19 August 2024
© King Abdulaziz City for Science and Technology 2024

Abstract

Diabetic mellitus (DM) is characterized by hyperglycaemia and defective macromolecular metabolism, arising from insulin resistance or lack of insulin production. The present study investigates the potential of artemisinin, a sesquiterpene lactone isolated from *Artemisia annua*, to exert anti-diabetic and antioxidant effects through modulation of the phosphoinositide 3-kinase (PI3K)/protein kinase B (AKT) signalling pathway. Our computational analyses demonstrated a high binding affinity of artemisinin with proteins belonging to the PI3K/AKT signalling cascade. α -Amylase and α -glucosidase studies revealed a notable increase in inhibition percentages with artemisinin treatment across concentrations ranging from 10 to 160 μ M. A similar significant ($p < 0.05$) dose-dependent inhibition of free radicals was observed for the in vitro anti-oxidant assays. Further, toxicological profiling of artemisinin in the in vivo zebrafish embryo-larvae model from 4 to 96 h post-fertilization (hpf) did not exhibit any harmful repercussions. In addition, gene expression investigations confirmed artemisinin's potential mechanism in modulating hyperglycaemia and oxidative stress through the regulation of the PI3K/AKT pathway. Overall, our investigation suggests that artemisinin can be used as a therapeutic intervention for diabetes and oxidative stress, opening up opportunities for future investigation in clinical settings.

Keywords Artemisinin · Oxidative stress · Anti-diabetic · Anti-oxidant · Toxicity · Zebrafish larvae

Introduction

Diabetes mellitus (DM) is characterized by hyperglycaemia due to distortion in insulin resistance or production (Pedersen-Bjergaard and Thorsteinnsson 2017). DM affects millions of individuals worldwide and remains a significant global health concern (Teo et al. 2021). Due to the rise in the prevalence of DM over the past 10 years, as well as the costly and detrimental side effects of modern medications, researchers are looking for innovative approaches to the treatment of diabetes (Yedjou et al. 2023). The upregulation of reactive oxygen species (ROS) in the body is one of the markers for DM (Lennicke and Cochemé 2021). ROS are natural by-products of cellular metabolism, which include superoxide, hydrogen peroxide (H_2O_2) and hydroxyl radicals. When they are upregulated, they become highly reactive and damage lipids, proteins, and DNA (Nakamura and Takada 2021). Notably, a link has been identified between DM and the upregulation of oxidative stress, which is suspected to have a crucial part in the furtherance of insulin sensitivity. This ROS plays a key part in the worsening the

✉ Praveen Kumar Issac
praveenkumari.sse@saveetha.com

¹ Institute of Biotechnology, Department of Medical Biotechnology and Integrative Physiology, Saveetha School of Engineering, Saveetha Institute of Medical and Technical Sciences, Thandalam, Chennai, Tamil Nadu 602 105, India
² Institute of Bioinformatics, Department of Computational Biology, Saveetha School of Engineering, Saveetha Institute of Medical and Technical Sciences, Thandalam, Chennai, Tamil Nadu 602 105, India
³ Department of Chemistry, College of Science, King Saud University, P.O. Box 2455, Riyadh 11451, Saudi Arabia
⁴ Department of Zoology, College of Science, King Saud University, P.O. Box - 2454, Riyadh 11451, Saudi Arabia
⁵ Department of Cariology, Saveetha Dental College and Hospitals, Saveetha Institute of Medical and Technical Sciences, Saveetha University, Chennai, India

insulin sensitivity, also contributing to neuronal death and neuronal dysfunction (Singh et al. 2022). It is also reported that oxidative stress contributes to both hypertensive diseases of pregnancy and gestational DM, resulting in insufficient placental perfusion and inflammation (Phoswa and Khaliq 2021). Furthermore, a study in skeletal muscle cells reported that lowering oxidative stress could improve insulin sensitivity in polycystic ovarian syndrome patients (Yao et al. 2022). Literature studies highlighted that the phosphoinositide 3-kinase (PI3K)/protein kinase B (AKT) signalling pathway plays a pivotal role in cellular processes, including glucose metabolism, antioxidant enzyme production, proliferation, and survival, which makes it a crucial target for therapeutic intervention in diabetes (Camaya et al. 2022).

In the pursuit of novel therapeutic options to treat oxidative stress and diabetes, natural products have raised considerable attention for their potential pharmacological benefits (Kamaraj et al. 2023). Extracts of *Symphytum officinale* and *Artemisia abrotanum* have been shown to have the potential against DM due to their inhibitory effects on digestive enzymes (Neagu et al. 2023). *Artemisia* species offers prospects as a therapeutic option for diabetes therapy and control due to its bioactive components, which successfully decrease blood glucose levels while having fewer side effects than conventional anti-diabetic medicines (Sharafati-Chaleshtori et al. 2021). *Artemisia annua* L. extracts reduced the insulin resistance by lowering lipid levels and adipocytokines in diabetic rats (Ghanbari and Sadeghimahalli 2022). Dicafeoylquinic acids of *Artemisia annua* L. leaves exhibit promising therapeutic benefits against diabetes and its consequences, by blocking enzymes and increasing wound healing (El-Askary et al. 2022). Another study on *Artemisia annua* L. extracts has reported significant antioxidant activity than metformin in the treatment of oxidative stress and liver dysfunction in diabetic mice (Ghanbari et al. 2023). Artemisinin, a sesquiterpene lactone derived from *Artemisia annua*, is traditionally recognized for its potent antimalarial activity throughout the world (Su and Miller 2015).

Our goal is to elucidate the antidiabetic and antioxidant attributes of artemisinin, with a specific focus on its modulation of the PI3K/AKT signalling pathway. Utilizing in silico methodologies like molecular docking, this study aims to computationally investigate the interactions between artemisinin and key components of the PI3K/AKT signalling cascade. Cell-free in vitro analysis was also carried out in this study to examine the anti-diabetic and anti-oxidant effects. Moreover, we employed in vivo toxicity assessment in this investigation to examine the safety profile of artemisinin. We also examined the expression of antidiabetic and antioxidant genes in stress-induced zebrafish larvae to evaluate the regulation of the PI3K/AKT pathway after artemisinin treatment.

While its therapeutic potential is promising, a thorough examination of its safety profiling will help to discover any adverse effects that may hinder its clinical translation. By elucidating its interactions with the PI3K/AKT signalling pathway, this study aims to provide mechanistic insights into its therapeutic potential, thereby contributing to the development of novel therapeutic interventions for diabetes mellitus and related complications.

Materials and methods

Artemisinin (ART) (Abcam, CAT No - ab141308), H₂O₂ (Thermo Scientific, CAT No - Q15465), α -amylase (SRL, CAT No - 95,114), α -glucosidase (SRL, CAT No - 75,551), Starch (SRL, CAT No - S9765), Calcium chloride (CaCl₂) (SRL, CAT No - 97,080), Tris HCl (SRL, CAT No - 99,438), Acarbose (SRL, CAT No - 65,457), P-nitrophenyl- α -D-glucopyranoside (SRL, CAT No - 12,735), 2,2-Diphenyl-1-Picrylhydrazyl (DPPH) (SRL, CAT No - 29,128), 2,2'-azino-bis(3-ethylbenzothiazoline-6-sulfonic acid (ABTS) (SRL, CAT No - 28,042), Trolox (OTTO, CAT No - T7723), Potassium persulfate (SRL, CAT No - 48,319), Sodium Chloride (SRL, CAT No - 33,205), Potassium chloride (KCl, SRL, CAT No - 84,984), Sodium phosphate dibasic (SRL, CAT No - 21,669), Potassium phosphate monobasic (SRL, CAT No - 54,358), Nitro blue tetrazolium (NBT) (SRL, CAT No - 11,207), Nicotinamide adenine dinucleotide (SRL, CAT No - 54,941), Phenazine methosulphate (OTTO, CAT No - P1485), Sodium nitroprusside (SRL, CAT No - 71,750), Griess reagent (SRL, CAT No - 35,657), Dimethyl sulfoxide (DMSO) (SRL, CAT No - 28,580), Trio™ Reagent (HiMedia, CAT No - MB566), AURA 2× One-Step RT-PCR Master Mix (Aura Biotech, ABT-018S).

In silico antidiabetic and antioxidant analysis

The in silico studies have been carried out on the personal computer (PC) with the Windows 11 (64-bit) operating system using the Intel Core™ i5 10th generation processor, 8 GB RAM and 512 GB SSD. Uniprot and RCSB PDB have been used to identify and retrieve the 3D structure of the proteins. Drug's 3D structure was downloaded from the PubChem database. The preparation of the proteins and ligands has been carried out with the AutoDock tools. The docking studies were performed using the AutoDock Vina software. The visualisation of the drug-protein interactions has been observed using the Accelrys Discovery Studio Visualizer.

Preparation of proteins

Based on the literature review, the insulin receptor (IR), Glycogen synthase kinase-3 Beta (GSK3- β), Phosphoinositide-dependent kinase-1 (PDK1), Phosphoinositide 3-kinases (PI3K), Protein kinase B (AKT) with the PDB (Protein Data Bank) Id's 1IR3, 1I09, 3RWQ, 3S2A, 8Q61, respectively, were chosen to study the antidiabetic activity, and Superoxide dismutase (SOD), Catalase (CAT), Glutathione synthase (GS), Glutathione peroxidase (GPx), Glutathione S-transferases (GST), Glutathione reductase (GR) with the PDB Id's 5VF9, 1DGF, 2HGS, 2F8A, 1GUM, 1XAN, respectively, were chosen to study the antioxidant activity of artemisinin. Their 3D structures were downloaded from PDB and saved for further studies (Ekambaram et al. 2021).

Preparation of ligand

The three-dimensional structure of the drug artemisinin (PubChem CID - 68,827) was retrieved from the PubChem database and the ligand was prepared for docking using the AutoDock tools and the "Add hydrogens" option was used to analyse the fidelity of the drugs. Then the drug was saved in PDB file format for further studies (Sathish Kumar and Kannan 2021).

Docking

The computational analysis of the antidiabetic and antioxidant activity of the artemisinin was performed by using the open-source software AutoDock vina. The water molecules in the proteins were removed from them and polar hydrogen atoms were added by selecting the "add polar" option. Then, the Kollman charges were introduced and the proteins were saved in Pdbqt format. The ligand molecules were also converted into Pdbqt file format. Based on the literature review, the binding regions, active site and catalytic site were listed and the docking was performed by creating a grid box which comprises the active sites or pockets. The binding affinity between the proteins and ligand was generated and based on the results the protein and ligand complex file was generated. The protein and ligand complex file were used to visualize the protein–ligand interactions under the discovery studio visualizer (Balakrishnan et al. 2022).

ADMET predictions

The computational ADME prediction of the drug artemisinin has been performed by using the SwissADME web server. The significant physiochemical properties of the drug were also checked for the possibility of considering it as a

potential lead. The toxicity and drug safety profiling were also checked by implementing the Lipinski rule (Anza et al. 2021).

In vitro antidiabetic and antioxidant analysis

α -Amylase inhibition assay

The α -amylase inhibition potential of the drug artemisinin was determined by using a substrate solution prepared by dissolving 2 mg of starch in 0.01 M CaCl_2 and 0.5 M Tris HCl, and then they were boiled and preincubated at room temperature for 5 min. Then, the positive control acarbose (160 μM) and artemisinin were added to the substrate solution at various concentrations (10, 20, 40, 80 and 160 μM), followed by pancreatic amylase. The reaction mixture was centrifuged at 4000 rpm for 10 min and the supernatant was used to measure the absorbance at 595 nm (thermo scientific) (Sudhakaran et al. 2023).

α -Glucosidase inhibition assay

The α -glucosidase inhibition potential of the drug artemisinin was determined by using a previously reported method with a few minor modifications (Dej-adisai et al. 2021). Acarbose (160 μM) and the drug artemisinin were added in various concentrations (10–160 μM) into the reaction mixture containing α -glucosidase (1 U/ml) and 100 mM phosphate buffer. The reaction mixture was preincubated for 15 min at room temperature and further incubated for 20 min after the substrate 5 mM P-nitrophenyl- α -D-glucopyranoside was added to the reaction mixture. The absorbance was measured at 405 nm after the reaction was stopped by using 0.1 M sodium carbonate.

DPPH assay

The DPPH assay was performed with a few modifications (Le et al. 2022). A 300 μM DPPH solution was mixed with Trolox (160 μM) and artemisinin (10–160 $\mu\text{M}/\text{ml}$) in an ELISA (enzyme-linked immunosorbent assay) plate. The plates were incubated in the dark for 30 min. Then, the samples were quantified at 517 nm using a microplate (96 well plate) reader.

ABTS assay

The ABTS assay was performed with a few modifications (Zampini et al. 2010). The ABTS solution was made by dissolving the 7 mM ABTS salt in 2.45 mM potassium persulfate. Then it was diluted with 0.2 M phosphate buffer saline (PBS) until it achieved 0.7 absorbance at 734 nm. Then, it was mixed with Trolox (160 μM) and artemisinin

(10–160 $\mu\text{M}/\text{ml}$) in an ELISA plate and incubated for 60 min in the dark at room temperature. After 60 min, the samples were quantified at 734 nm using a microplate (96-well plate) reader and the percentage of inhibition was calculated.

H₂O₂ scavenging assay

The H₂O₂ scavenging assay was performed with a few modifications (Alam et al. 2013). The reaction mixture was prepared by adding 40 mM H₂O₂ in 50 mM phosphate buffer. Then the reaction mixture was mixed with Trolox (160 μM) and artemisinin (10–160 $\mu\text{M}/\text{ml}$) and incubated in the dark for 10 min. After incubation, the absorbance was measured at 230 nm and the percentage of inhibition was calculated.

Superoxide (O₂^{•-}) radical scavenging assay

The O₂^{•-} radical scavenging assay was performed as previously described with a few modifications (Balamurugan et al. 2008). The reaction mixture was prepared by adding 50 μM NBT, 15 μM phenazine methosulfate, 73 μM nicotinamide adenine dinucleotide and 20 mM phosphate buffer. Then, the reaction mixture was mixed with Trolox (160 μM) and artemisinin (10–160 $\mu\text{M}/\text{ml}$) and incubated in the dark for 5 min. After the end of the incubation process, the absorbance was measured at 562 nm.

Nitric oxide (NO) scavenging assay

The NO scavenging potential of artemisinin was estimated by using the Griess method with a few modifications (Nisa et al. 2023). The reaction mixture was prepared by making 10 mM Sodium nitroprusside using 1X phosphate buffer saline. Then, the Griess reagent was added followed by Trolox (160 μM) and artemisinin (10 to 160 $\mu\text{M}/\text{ml}$) and incubated for 25 min. The inhibitory percentage of nitric oxide was measured at 546 nm.

In vivo toxicity analysis

Zebrafish maintenance and treatment

Both male and female adult zebrafish were acquired from the Tarun fish farm, Manimangalam, Chennai. The fish are maintained by following the rules and regulations suggested by the ethical committee of the institution (SU/CLAR/RD/001/2023). They are kept in a 3 L tank at a temperature of around 28 °C and maintained in a light/dark cycle of 14/10 h. They were fed with live brine shrimps and allowed to acclimatize for 2 weeks. The breeding groups were kept in a 2:1 ratio (male: female) and the eggs were collected after spawning. The embryos were segregated by microscopic

observation and the fertilized embryos were kept in an embryo medium for further studies.

Developmental toxicity assessment

To determine the toxicity induced by artemisinin (10–160 $\mu\text{M}/\text{ml}$), 3 h post-fertilisation (hpf) embryos were used. The larvae were divided into $n = 30/\text{group}$. The control groups were maintained in embryo media and 0.1% DMSO was used as a vehicle control (Surya et al. 2023).

Behavioural toxicity

The alterations in the locomotory behaviour of the larvae were checked using a method suggested by Krishnan et al., 2019 with a few changes (Krishnan and Kang 2019). Briefly, the larvae ($n = 3/\text{well}$) for each group were placed in a white ice cube tray with dimensions 2.5 × 3.5 cm. After a 10 min acclimatization period, the movement of the larvae was recorded in a noise-free environment and analysed using the UMA Tracker software.

Gene expression studies

The H₂O₂ was used to induce oxidative stress in the zebrafish embryo-larvae model up to 96 hpf. After the exposure period, the larvae were homogenized and the total RNA was extracted by using RDP Trio™ Reagent. The primers for PI3K, AKT, Nuclear factor erythroid 2-related factor 2 (NRF2), and CAT were designed using the NCBI's Primer-BLAST. The nucleic acid sequence of the primers is mentioned in Table 1. AURA 2 × One-Step RT-PCR Master Mix (AURA Biotechnologies Pvt Ltd., Ayanambakkam, Chennai) was used to analyse the expression of the genes. The one-step RT-PCR programming involves a series of steps to amplify the RNA sequences. The reverse transcription process begins with a single cycle lasting 15 min at temperatures ranging from 44 to 50 °C, followed by enzyme activation, which is performed once at a temperature of 95 °C for 3 min. Then, 40 cycles of denaturation for 10 s at 95 °C, annealing for 45 s at 60 °C, and finally, extension happens at 72 °C for 15 s was performed (Issac et al. 2020).

Statistics

All the data represented in this investigation were provided as mean \pm standard deviation. The data were analysed in GraphPad Prism 5.0 using the one-way analysis of variance (ANOVA) and Tukey multiple range test. The data were considered as significant and marked by the symbol “*” when $p < 0.05$.

Table 1 Nucleic acid sequences of primers used in zebrafish larvae antidiabetic and antioxidant gene study

S. No	Gene	Sequence	Reference
1	PI3K	GAGATTTTCTCGGCCCTGGCT ACTCTTCCCATCTGTGTGAGGC	NCBI: NM_001281844.1
2	AKT	GGCTATAAGGAGCGACCGCA GGTGCGCTCAATGACAGTGG	NCBI: NM_001281801.1
3	NRF2	CTCCAAACCTCCGTTACCA GTCGTCTACGGGCAGATTGA	NCBI: XM_005172511.4
4	CAT	AACTGTGGAAGGAGGGTCCG CGCTCTCGGTCAAAATGGGC	NCBI: XM_021470442.1
5	β -actin	AAGCTGTGACCCACCTCACG GGCTTGCACATACCGGAGC	NCBI: NM_131031.2

Table 2 Molecular docking scores of artemisinin with proteins involved in the PI3K/AKT signalling pathway

S. No	Protein	PDB ID	Score (kcal/mol)	Hydrogen bond
1	IR	1IR3	- 7.7	2
2	AKT	8Q61	- 8.6	1
3	GSK3- β	1I09	- 8.1	-
4	PDK1	3RWQ	- 8.4	2
5	PI3K	3S2A	- 7.7	1
6	SOD	5VF9	- 7.2	-
7	CAT	1DGF	- 9.0	1
8	GPx	2F8A	- 6.4	-
9	GS	2HGS	- 7.4	2
10	GST	1GUM	- 8.2	1
11	GR	1XAN	- 8.3	3

Results

In silico antidiabetic and antioxidant analysis

Docking analysis

The antidiabetic and antioxidant potential of artemisinin was determined by docking it against different proteins involved in the PI3K/AKT pathway and the docking scores are mentioned in Table 2. Among the proteins used for antidiabetic studies (Fig. 1A–E), artemisinin has a higher binding affinity of - 8.6 kcal/mol with AKT, followed by - 8.4 kcal/mol with PDK1, - 8.1 kcal/mol with GSK3- β , - 7.7 kcal/mol with both IR and PI3K. And among the proteins used for antioxidant studies (Fig. 2A–F), artemisinin has a higher binding affinity of - 9.0 kcal/mol with CAT, followed by - 8.3 kcal/mol with GR, - 8.2 kcal/mol with GST, - 7.4 kcal/mol with GS, - 7.2 kcal/mol with SOD, and -6.4 kcal/mol with GPx.

ADMET predictions

ADME (SwissADME) predictions revealed substantial physiochemical properties to be within the allocated range for consideration as a possible hit (Fig. 3). Further, the oral bioavailability rules like Lipinski rule of 5, Veber rule, Egan rule, Ghose rule, and Muegge rule were implemented and found to be fit with higher significance. The pharmacokinetics parameters were also evaluated to ensure drug safety, wherein the compound artemisinin was found to be safe with higher significance (Table S1–S5).

In vitro antidiabetic and antioxidant analysis

α -Amylase inhibition assay

The α -amylase study was employed to evaluate the anti-oxidant potential of the artemisinin. The positive control acarbose exhibited 90.9% of inhibition. Notably, artemisinin demonstrated a concentration-dependent α -amylase inhibition. Specifically, at 80 μ M, artemisinin significantly reduced α -amylase by 66.1% ($p < 0.05$), exhibiting substantial antidiabetic efficacy (Fig. 4A).

α -Glucosidase inhibition assay

The α -glucosidase study was employed to evaluate the anti-oxidant potential of the artemisinin. Here, artemisinin demonstrated concentration-dependent α -glucosidase inhibition capability, where the inhibition was observed as 20.9% at 10 μ M, 35.2% at 20 μ M, 55.9% at 40 μ M, 68.1% at 80 μ M, and 67.2% at 160 μ M when compared to the positive control acarbose with 90.4% inhibition ($p < 0.05$) (Fig. 4B).

DPPH scavenging assay

The DPPH scavenging study was employed to evaluate the anti-oxidant potential of artemisinin. The violet-coloured DPPH solution becomes colourless when reduced by an

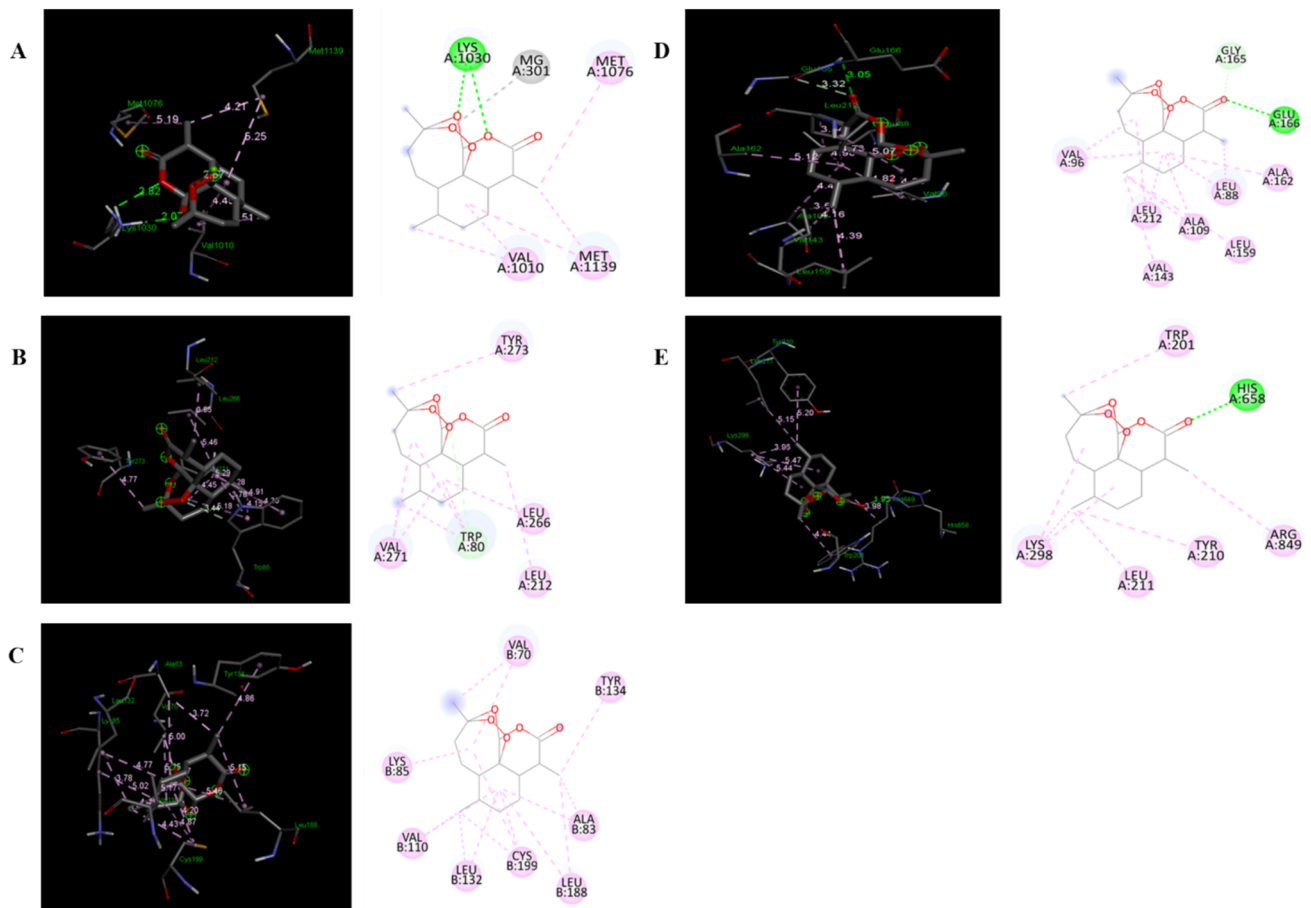


Fig. 1 Visualization of the three-dimensional (3D) and two-dimensional (2D) interactions between artemisinin and pivotal proteins involved in the PI3K/AKT signalling pathway: **A** IR, **B** AKT, **C** GSK3- β , **D** PDK1, and **E** PI3K. The interactions were analysed

using Discovery Studio Visualizer, illustrating the binding modes and potential molecular mechanisms underlying artemisinin's modulation of the PI3K/AKT pathway

anti-oxidant. Trolox was used as the positive control, which exhibited 92.5% of inhibition. Notably, artemisinin demonstrated a concentration-dependent antioxidant activity, with an IC_{50} value of 19.13 μ M. Specifically, at a concentration of 80 μ M, artemisinin significantly reduced the DPPH radical by 56.9% ($p < 0.05$), exhibiting substantial anti-oxidant efficacy (Fig. 5A).

ABTS + cation scavenging assay

The ABTS assay involves measuring the reduction of the blue-green chromophore ABTS⁺ by an anti-oxidant. Here, artemisinin demonstrated concentration-dependent ABTS radical scavenging capability, where the inhibition was observed as 25.1% at 10 μ M, 39.2% at 20 μ M, 54.7% at 40 μ M, 63.1% at 80 μ M, and 57.3% at 160 μ M when compared to the positive control Trolox with 94.5% inhibition ($p < 0.05$) (Fig. 5B). The IC_{50} value was calculated to be 21.52 μ M.

H₂O₂ scavenging assay

H₂O₂ can give rise to highly reactive hydroxyl radicals in a process known as the Fenton reaction, which can cause oxidative damage to various cellular components. The results indicate that artemisinin has a strong H₂O₂ scavenging property with an IC_{50} value of 33.81 μ M. The highest percentage of inhibition (53.1%) was observed at the 80 μ M concentration, which was significant when compared with Trolox (91.1%) (Fig. 5C).

Superoxide scavenging assay

Despite being a weak oxidant, the superoxide anion can create very strong hydroxyl radicals and singlet oxygen, causing oxidative stress. The superoxide scavenging assay was performed to evaluate the antioxidant potential of the artemisinin, with Trolox serving as the positive control. The superoxide radical scavenging activity of artemisinin was

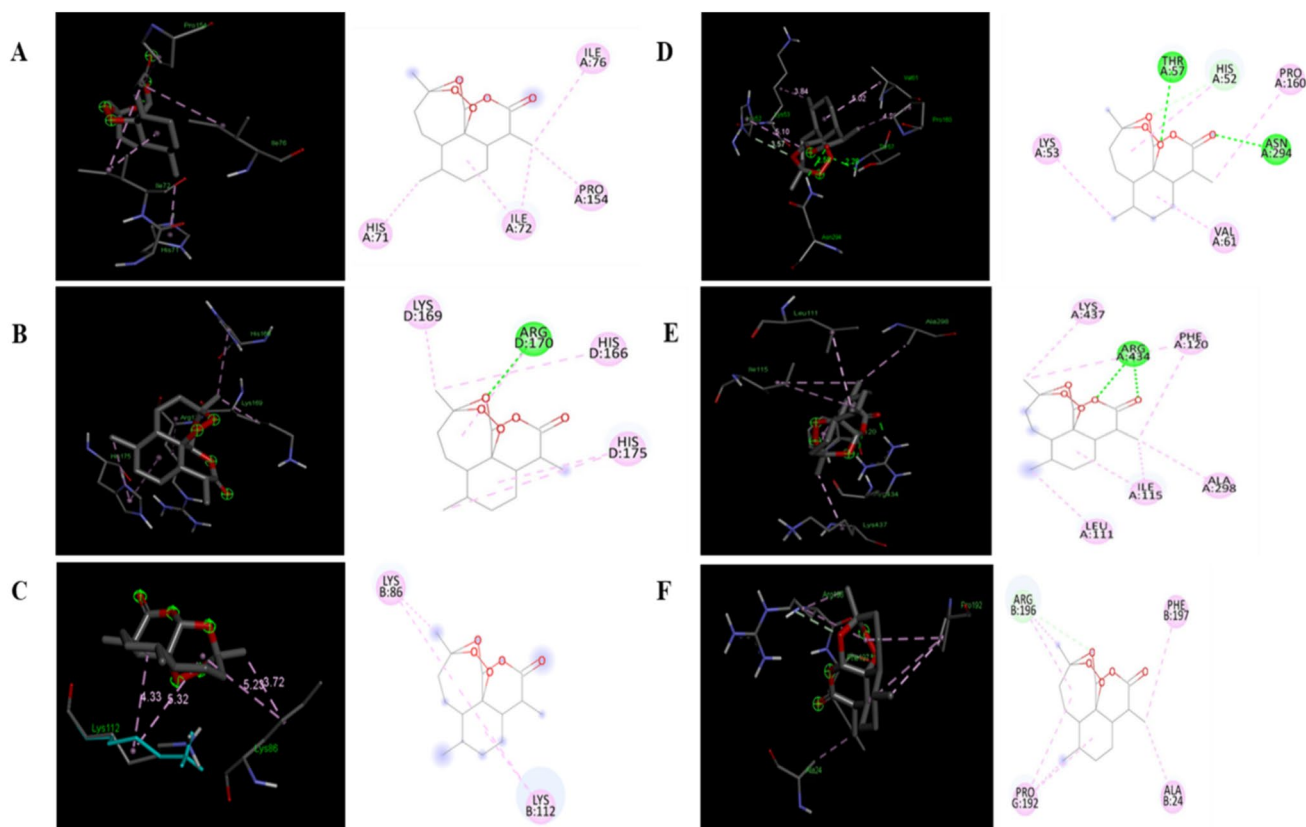


Fig. 2 Visualization of the three-dimensional (3D) and two-dimensional (2D) interactions between artemisinin and pivotal proteins involved in the PI3K/AKT signalling pathway: **A** SOD, **B** CAT, **C** GPx, **D** GR, **E** GS, and **F** GST. The interactions were analysed using

Discovery Studio Visualizer, illustrating the binding modes and potential molecular mechanisms underlying artemisinin’s modulation of the PI3K/AKT pathway

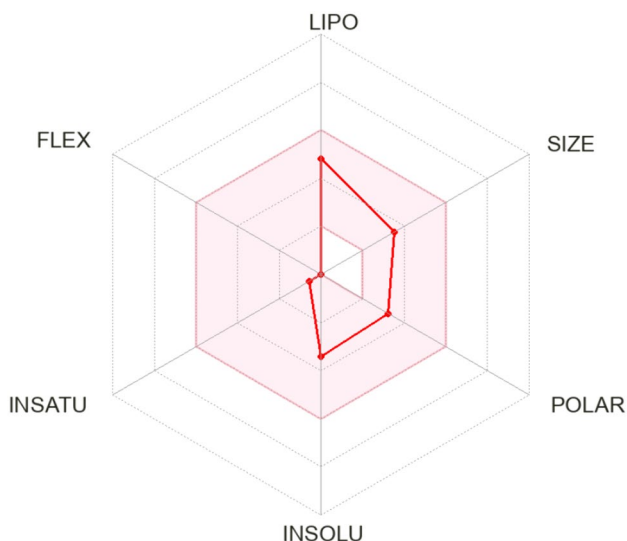


Fig. 3 Bioavailability radar plot generated using SwissADME to predict the pharmacokinetic parameters and drug-likeness properties of artemisinin. The radar plot provides a comprehensive visual representation of key molecular descriptors such as lipophilicity, water solubility, molecular weight, and pharmacokinetic parameters, aiding in the assessment of artemisinin’s potential as a drug candidate

observed to be concentration-dependent with an IC_{50} value of $24.16 \mu\text{M}$. Where $80 \mu\text{M}$ of artemisinin nanoparticles showed a substantial ($p < 0.05$) percentage of inhibition (54.1%) when compared with positive control (87.4%) (Fig. 5D).

NO scavenging assay

Nitric oxide can react with various molecules in the body and give rise to reactive nitrogen species. It also causes neurotoxicity and is involved in various neurodegenerative diseases. The NO assay evaluated the ROS neutralizing properties of the artemisinin at various concentrations. Among them, $80 \mu\text{M}$ showed a notable percentage of inhibition of about (52.45%) with a statistical significance of $p < 0.05$ when compared with the Trolox (94.4%). (Fig. 6).

In vivo toxicity analysis

Survival rate

The survival of zebrafish embryos exposed to artemisinin at concentrations of 10, 20, 40, 80 and $160 \mu\text{M}$ was

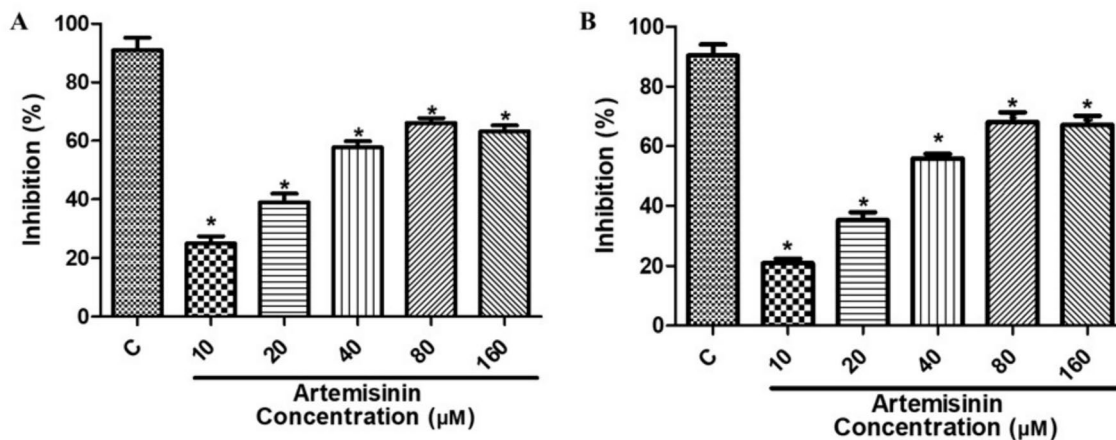


Fig. 4 The figure illustrates the dose-dependent inhibition activity of artemisinin at concentrations ranging from 10 to 160 μM on **A** α-amylase and **B** α-glucosidase enzymes, alongside comparative data with acarbose. Significant differences ($p < 0.05$) are denoted by asterisks (*).

isks (*). These findings highlight artemisinin's potential as an inhibitor of key enzymes involved in carbohydrate metabolism, suggesting its therapeutic relevance in managing hyperglycaemia

calculated (4–96 hpf). Artemisinin at lower concentrations (10, 20, 40 μM) does not account for significant mortality in zebrafish larvae (96 hpf). Conversely, larvae exposed to artemisinin at 80 and 160 μM showed a significant decrease in the number of zebrafish larvae survived ($n = 18 \pm 1.5$ and $n = 13 \pm 1$) ($p < 0.05$). Compared to the control, the mortality rate of artemisinin at concentrations of 10, 20, and 40 μM was not statistically significant (Fig. 7A).

Hatching rate

The hatching rate was estimated for all the groups (48 hpf). In the control group, all ($n = 30$) of zebrafish embryos emerged from their chorions. Similarly, the hatching rate was not altered in the lower concentrations (10, 20, 40 μM) exposed group. In contrast, the hatching rate decreased to $n = 22 \pm 1.5$ and $n = 16 \pm 1$ in the 80 and 160 μM exposure groups (Fig. 7B).

Heart rate

The cardiotoxicity of artemisinin-exposed zebrafish larvae was determined at 72 hpf. Under an electron microscope, atrium and ventricular impulses were recorded for 1 min, and the average of the heartbeat was calculated. In contrast to the control group larvae, which exhibited an average heart rate of 177 ± 2.1 beats per minute (bpm), those exposed to artemisinin at concentrations of 80 μM (160 ± 2.1 bpm) and 160 μM (152 ± 2.5 bpm) demonstrated a statistically significant reduction in heart rate. On the other hand, artemisinin at the lower concentrations (10, 20, 40 μM) had no impact on the normal function of the heart (Fig. 7C).

Developmental malformations

The zebrafish embryos and larvae exposed to control, 0.1% DMSO, and lower concentrations of artemisinin (10, 20, 40 μM) exhibited normal morphological structure from 4 to 96 hpf. However, the larvae treated with 80 and 160 μM showed bent tail (BT), yolk sac edema (YSE) and bent spine (BS). This proves that the embryo exposed to the artemisinin did not exhibit any lethal developmental morbidity (Fig. 8A–C).

Behavioural toxicity

The zebrafish larvae locomotory analysis is a sensitive method for measuring the consequences of oxidative stress on locomotory activity. The oxidative stress-induced zebrafish larvae were treated with 0.1% DMSO, and artemisinin (10, 20, 40, 80, and 160 μM) and their movements were analysed. The cognitive function was measured by using the distance travelled by the larvae (meters). The 80, and 160 μM groups showed reduced movement (28.12 ± 7.1 , 11.08 ± 4.8) with an abnormal pattern. Among the treatment groups, the distance travelled by the larvae was recorded to be 72.1 ± 4.2 for 10 μM, 60.9 ± 9 for 20 μM and 44.3 ± 4.5 for 40 μM. These results suggest that artemisinin at lower concentrations has better locomotory patterns with a more normal state (Fig. 9A–H).

Gene expression

The expression of antidiabetic and antioxidant genes in the oxidative stress-induced zebrafish larvae treated with artemisinin was examined. The amplification plot was plotted

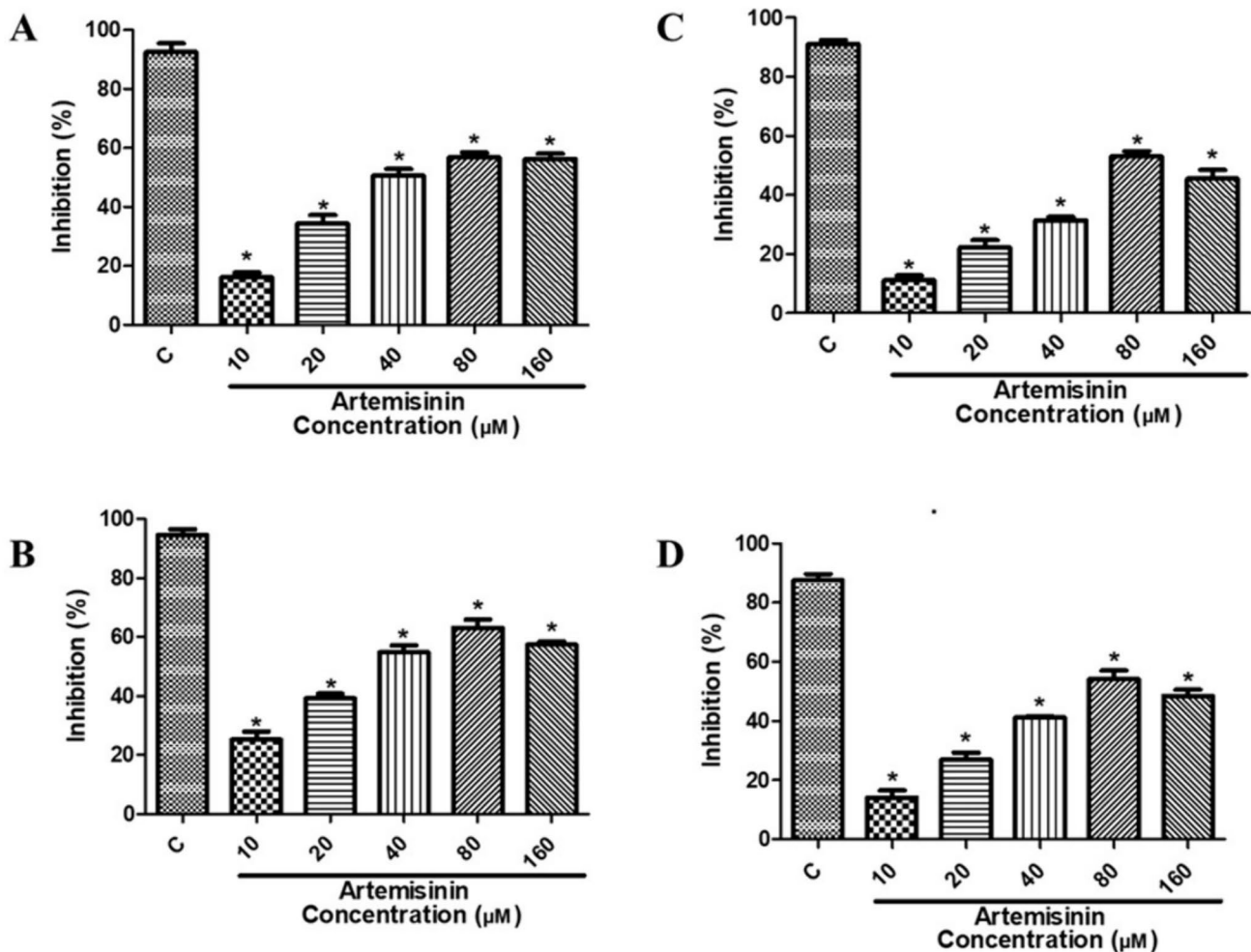


Fig. 5 It depicts the antioxidant activity of artemisinin at concentrations ranging from 10 to 160 μM against various reactive oxygen species: **A** DPPH (2,2-diphenyl-1-picrylhydrazyl), **B** ABTS (2,2'-azino-bis(3-ethylbenzothiazoline-6-sulfonic acid)), **C** H₂O₂, and

(D) superoxide radicals, in comparison with trolox as a reference antioxidant. Significant differences ($p < 0.05$) are indicated by asterisks (*), underscoring artemisinin's potential as a potent antioxidant compound across different assays

(Fig. S1) and the relative fold difference in the gene expression was calculated to evaluate the impact of H₂O₂-induced oxidative stress and treatment with artemisinin in the zebrafish larvae via the PI3K/AKT pathway. When compared to the control, the H₂O₂-treated group showed a significant reduction in the expression of all the antidiabetic and antioxidant genes, PI3K (0.3 fold), AKT (0.3 fold), NRF2 (0.3 fold) and CAT (0.4 fold). However, when compared to the control the expression of PI3K (1.6 fold), AKT (1.8 fold), NRF2 (1.7 fold) and CAT (2.4 fold) were significantly ($p < 0.05$) upregulated in the artemisinin treated group (Fig. 10).

Discussion

Free radicals are short-lived, reactive chemical molecules with unpaired electrons. The free radicals are generally classified as reactive chlorine species (RCS), reactive nitrogen species (RNS) and reactive oxygen species (ROS). They play a crucial role in signalling pathways like MAPK and ERK pathways, which alter gene expression. However, the upregulation of free radicals may lead to cell death and tissue damage. Studies also reported that free

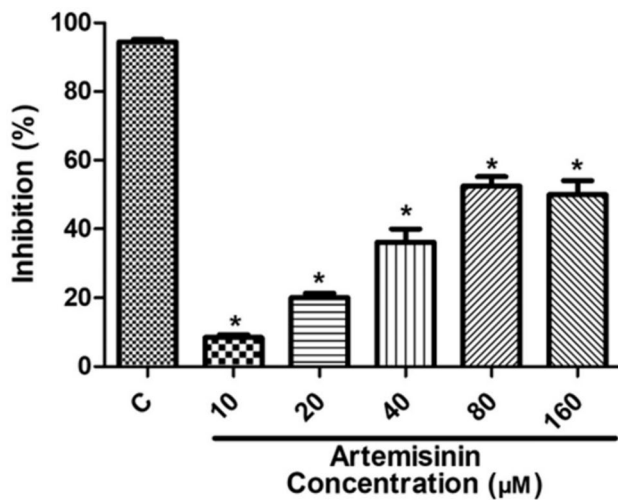


Fig. 6 The assessment of nitric oxide (NO) scavenging potential of artemisinin at concentrations ranging from 10 to 160 µM, alongside comparison with Trolox as a standard antioxidant. Significant differences ($p < 0.05$) are denoted by asterisks (*). These results highlight artemisinin's ability to scavenge NO, suggesting its potential therapeutic application in managing oxidative stress-related conditions

radical upregulation may lead to vascular complications in type 2 diabetes mellitus (Asmat et al. 2016). Reports suggest that the upregulation of free radicals in type 2 diabetes mellitus is caused by mitochondria. It is observed that during energy metabolism the mitochondria release superoxide ($O_2^{\bullet-}$) as an undesirable by-product, which leads to the generation of other forms of free radicals. Those free radicals in turn negatively regulate insulin signalling by increasing insulin sensitivity and may lead to insulin resistance (Pizzino et al. 2017). Recently, plant secondary metabolites have grabbed a lot of attention for their wide range of therapeutic potential, including antioxidant and antidiabetic properties (Shori 2015). Artemisinin, a sesquiterpenoid isolated from the plant *Artemisia annua*, is reported to have antimalarial properties (Klayman 1985). In this research, the in silico and in vitro antidiabetic and antioxidant properties of artemisinin were explored, followed by an analysis of the developmental and behavioural toxicity induced by artemisinin exposure in the in vivo model.

In this investigation, we examined the potential of artemisinin against the proteins involved in the PI3K/AKT

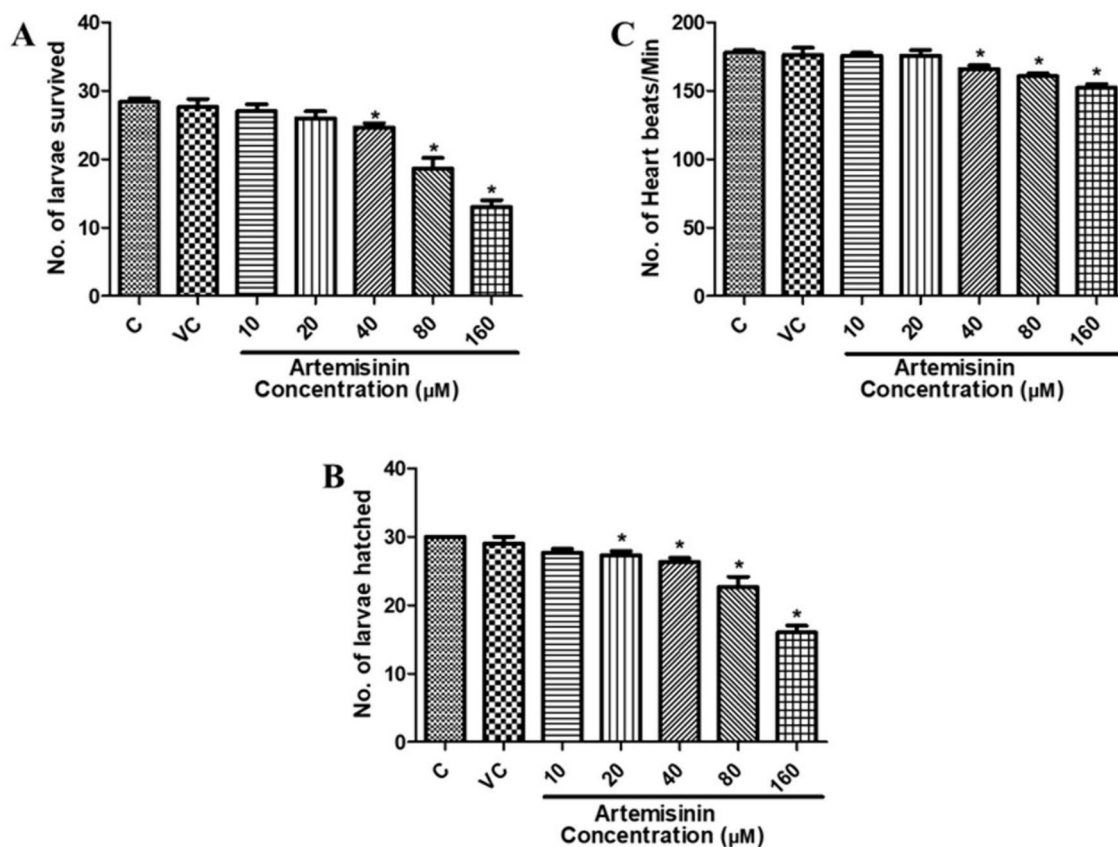
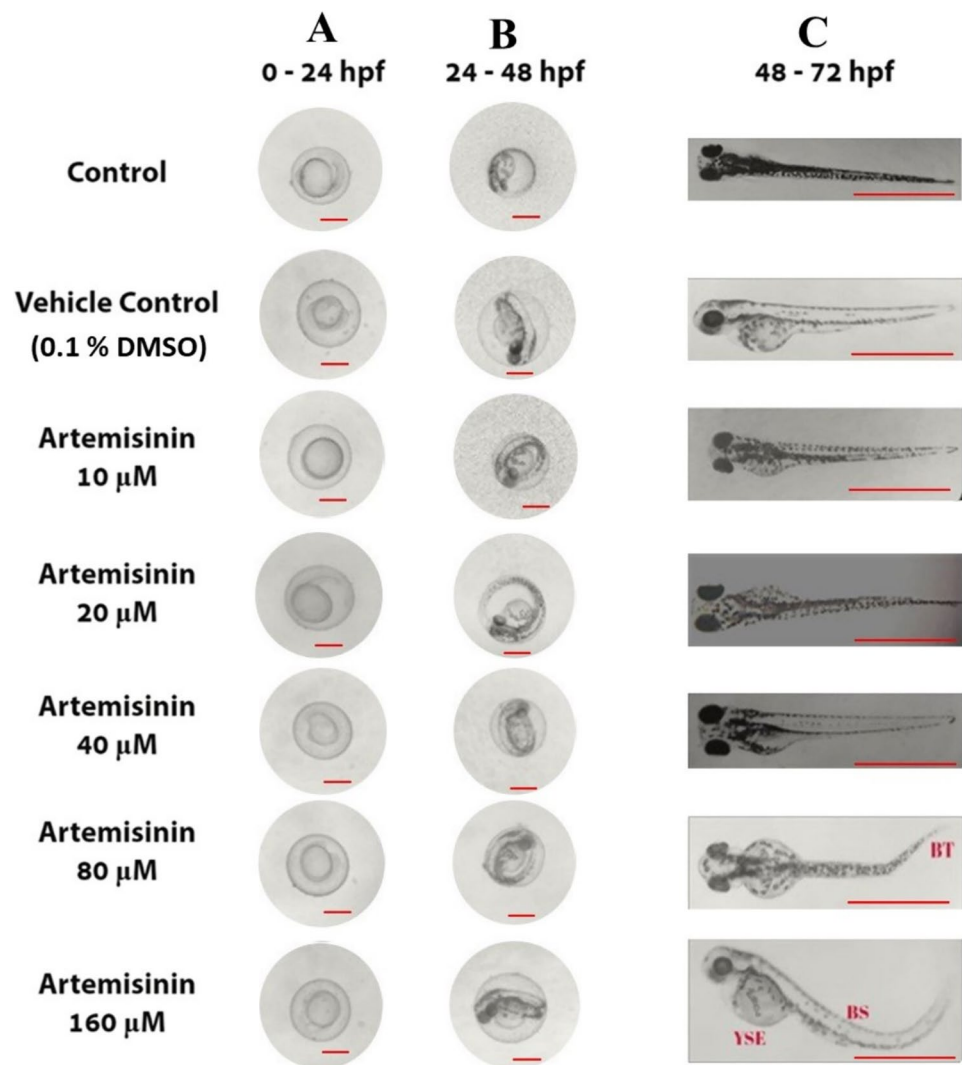


Fig. 7 The figure displays the outcomes of the assessment on zebrafish larvae, including **A** survival rate over a period from 4 to 96 h post-fertilization (hpf), **B** hatching rate at 48 hpf, and **C** heart

rate at 72 hpf. Significant differences ($p < 0.05$) are indicated by asterisks (*), emphasizing the effects of artemisinin exposure on these developmental and physiological parameters

Fig. 8 In vivo developmental analysis of zebrafish embryos exposed to artemisinin included **A** embryos at 24 h post-fertilization (hpf, Gastrula stage) with a scale of 25 μm , **B** embryos at 48 hpf (organogenesis stage) with a scale of 25 μm , and **C** larvae at 72 hpf stage with a scale of 100 μm . The control and treatment groups (10–40 μM) showed no lethal malformations, whereas the 80 μM and 160 μM treatment groups exhibited lethal malformations such as bent tail (BT), yolk sac edema (YSE), and bent spine (BS)



pathway to screen its antidiabetic and antioxidant properties. The selected proteins were docked against artemisinin using AutoDock Vina. All the PI3K/AKT signalling pathway proteins evaluated in this study have been reported with significant binding affinity. Among the proteins selected for the antidiabetic study of artemisinin, AKT (8Q61) showed the highest binding affinity of -8.6 kcal/mol. This strong interaction was facilitated by the formation of 1 hydrogen bond (TRP 80) and complemented by 11 hydrophobic interactions (LEU 226, VAL 271, LEU 212, TRP 80, and TYR 273). Notably, among these interactions, four hydrophobic interactions are involved with VAL 271 and TYR 273, where the region between VAL 272 and LEU 283 is crucial for the kinase's catalytic activity. Furthermore, the TRP 80 is also reported to be one of the important residues involved in the ligand binding to AKT (Zhong and Goodwin 2024). Among the proteins selected for the antioxidant study of artemisinin, CAT (1DGF) showed the highest binding affinity of -9.0 kcal/mol with 1 hydrogen

bond (ARG 170) and 5 (ARG 170, LYS 169, HIS 166, and HIS 175) hydrophobic interactions. An investigation on the root extract of *A. chinensis* Planch to understand its pharmacological mechanism reported a similar binding between the HIS 175 residue and (+)-catechin (Hu et al. 2022). The ADMET characteristics of artemisinin were predicted by using the SwissADME, which demonstrated promising drug-likeness, pharmacokinetic characteristics and medicinal chemistry attributes. The Lipinski rule of 5, indicates that artemisinin meets all the necessary criteria without any violations with favourable ADME properties. Furthermore, artemisinin satisfied all the physiological parameters of other models like Ghose, Veber, Egan, and Muegge for therapeutic effectiveness. It was also predicted with high gastrointestinal absorption, and the ability to penetrate the blood–brain barrier (BBB), along with a bioavailability score of 0.55. While artemisinin does not significantly inhibit numerous cytochrome P450 (CYP) enzymes important in drug metabolism, it does

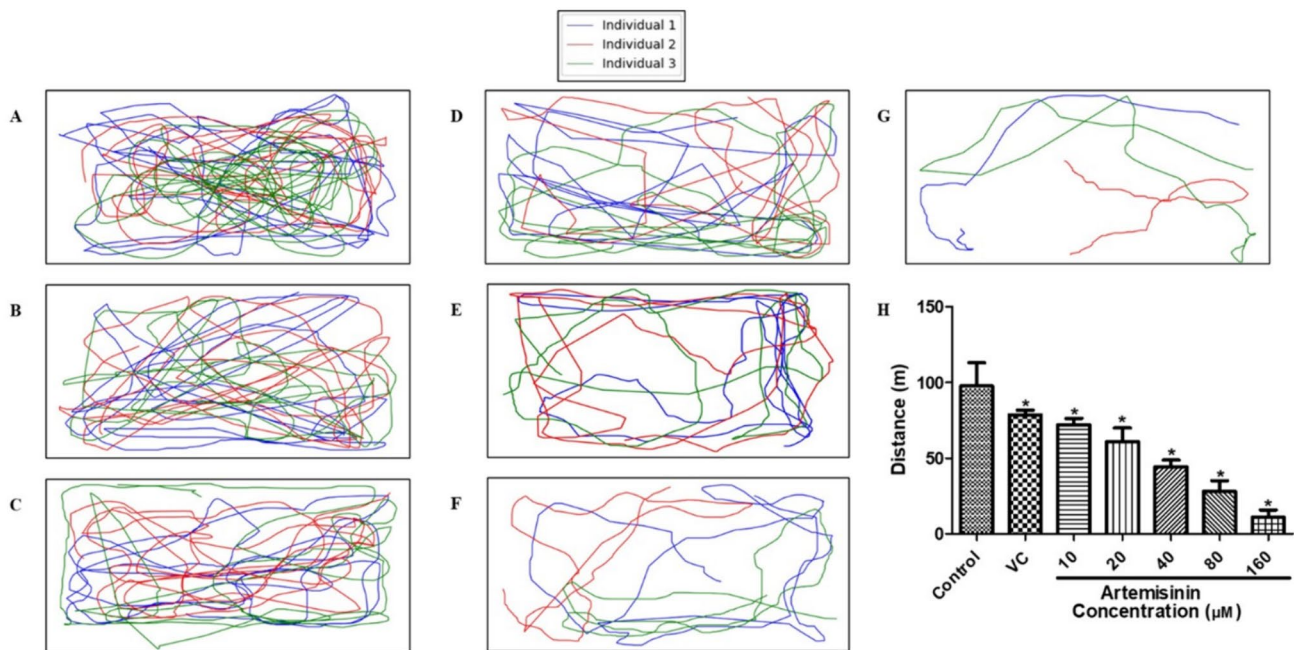
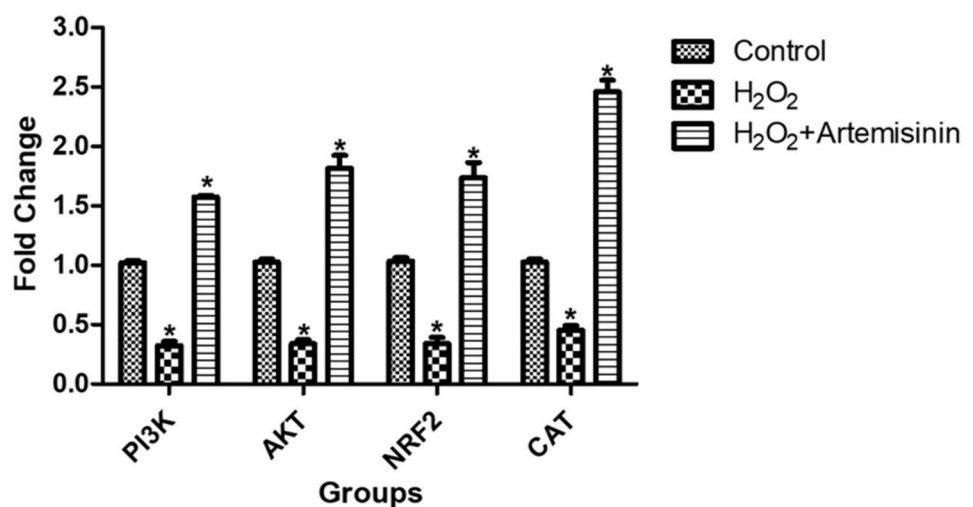


Fig. 9 Behavioural tracking of zebrafish larvae treated with **A** Control, **B** Vehicle control, **C** 10 μM , **D** 20 μM , **E** 40 μM , **F** 80 μM , and **G** 160 μM of artemisinin, illustrating their movement patterns. **H** Distance travelled by larvae. Significant differences ($p < 0.05$)

are denoted by asterisks (*). This analysis provides insights into the effects of artemisinin on the behaviour of larvae under oxidative stress conditions

Fig. 10 The figure presents the assessment of artemisinin's impact on antidiabetic and antioxidant gene expression in zebrafish larvae induced with oxidative stress at 96 hpf. Significant differences ($p < 0.05$) are denoted by asterisks (*), highlighting the potential regulatory effects of artemisinin on genes involved in glucose metabolism and oxidative stress response pathways



inhibit CYP1A2. Although one alert is raised in medicinal chemistry assessment regarding its peroxide group, this feature is intrinsic in artemisinin's structure and therapeutic property. Similar issues in the pharmacokinetics and medicinal chemistry assessments have been observed during the investigation of the ADMET properties of Nimbin analogues. Despite these challenges, in vitro studies on L6 myotubes demonstrated a significant upregulation of proteins involved in the PI3K/AKT signalling pathway (Sudhakaran et al. 2023). This upregulation indicates a

potential mechanism through which Nimbin analogues exert their biological effects, particularly in promoting cell growth and survival. The findings suggest that while there may be hurdles in optimizing the pharmacokinetic profiles of these compounds, their ability to modulate crucial signalling pathways remains promising for therapeutic applications.

The in vitro antidiabetic and anti-oxidant assays were used to assess artemisinin's antidiabetic and antioxidant capacity. The α -amylase inhibition assay measures the ability of a compound to inhibit the activity of alpha-amylase, an

enzyme that breaks down complex carbohydrates (starch) into simpler sugars (maltose). The α -glucosidase assay assesses the ability of a compound to inhibit α -glucosidase, an enzyme responsible for breaking down disaccharides (maltose) into monosaccharides (glucose) (Singh et al. 2021). A dose-dependent increase in the inhibition of α -amylase and α -glucosidase ($p < 0.05$) was recorded, demonstrating the significant potential of the tested compounds in modulating these key enzymes involved in carbohydrate metabolism. Similar results have been observed in extracts of *Adiantum caudatum* Linn. and *Celosia argentea* Linn., as reported by Hullatti and Telagari (2015) (Hullatti and Telagari 2015). These findings highlight the consistent efficacy of natural plant extracts in enzyme inhibition, suggesting their potential use in managing conditions such as diabetes mellitus by regulating postprandial blood glucose levels. The parallel between the current study and previous research underscores the importance of exploring diverse botanical sources for bioactive compounds with therapeutic applications. In the DPPH assay, antioxidants reduce the DPPH radical, and result in a colour change that can be quantified spectrophotometrically, whereas the ABTS assay evaluates the antioxidant's potential to neutralise the ABTS radical cation. Furthermore, the H_2O_2 scavenging assay examines the ability of antioxidants to break down H_2O_2 , whereas the superoxide scavenging assay measures the antioxidant's ability to neutralise superoxide radicals (Kotha et al. 2022). These in vitro analyses provide understanding into the aspects of artemisinin's potential to reduce oxidative stress by scavenging different forms of free radicals. A dose-dependent upregulation in the inhibition percentage from 10 to 160 μ M concentration of artemisinin was noted in all the in vitro anti-oxidant assays. The 80 μ M showed a higher percentage of inhibition with significant $p < 0.05$ when compared with Trolox. These findings align well with the work of Lalhminghlui and Jagetia (2018), who found a similar dose-dependent inhibitory profile, across different solvent extracts of *S. wallichii*, including chloroform, ethanol, and aqueous extracts (Lalhminghlui and Jagetia 2018). The NO scavenging assay evaluates the drug's ability to neutralise the rapidly reactive nitric oxide radical. In biological systems, nitric oxide functions as both a signalling molecule and an oxidative stress mediator (Theivendran et al. 2022). The NO scavenging assay revealed a concentration-dependent response for artemisinin in the scavenging of NO. The percentage of NO inhibition at different concentrations of artemisinin demonstrates its capacity to regulate excess NO radicals. The concentration of 80 μ M showed increased NO scavenging activity ($p < 0.05$). The potential of artemisinin to scavenge NO radicals suggests that they will be used to treat oxidative stress-induced insulin sensitivity. Our findings align with a comprehensive study on the bioactive profile of *Camellia*

japonica flowers. They revealed a notable dose-dependent reduction in NO levels while evaluating their in vitro antioxidant properties. The investigation included both pink and white phenotypes from various cultivars, highlighting a consistent trend across different genetic backgrounds (Pereira et al. 2024).

Zebrafish in the early embryonic stages (4–96 hpf) are more vulnerable to xenobiotic exposure than larvae and adults. Zebrafish embryos have morphological, psychological, and functional similarities with humans (Sant and Timme-Laragy 2018). The zebrafish embryo and larvae model were used for the in vivo experimental studies. The artemisinin concentrations in this study were selected based on a preparatory study between concentrations 10 and 250 μ M. The concentrations above 160 μ M showed toxic effects and hence the concentrations between 10 and 160 μ M were chosen for this study. The survival, heart rate, hatching and developmental deformation of the embryo-larvae model under the influence of artemisinin have been studied. Our study noted that the hatching and survival rate was reduced in the treatment groups above 40 μ M when compared with the control group. The hatching and survival rate of the artemisinin-treated group at lower concentrations (10, 20, 40 μ M) was significant ($p < 0.05$) when compared with the control group. The heart is among the earliest organs to form in zebrafish embryos and continues to operate throughout development (Echeazarra et al. 2021). Across the tested range of artemisinin exposures (10–160 μ M), no statistically significant decreases in heart rate were noted in zebrafish larvae treated with concentrations up to 40 μ M. However, concentrations exceeding 40 μ M exhibited a significant reduction in heart rate, suggesting the onset of non-lethal stress effects. Notably, non-lethal morphological malformations such as bent tail, yolk sac edema, and bent spine were observed in larvae exposed to 80 and 160 μ M concentrations after 3 days post-fertilization (dpf). These non-lethal effects are consistent with previously reported outcomes in the literature for vitellogenin exposure in in vivo embryo–larvae models (Dambal et al. 2017). Notably, the larvae exposed to lower concentrations of artemisinin (10, 20, and 40 μ M) did not reveal any lethal malformations. This suggests that while artemisinin can be tolerated at lower concentrations, higher exposures may induce stress responses and developmental abnormalities, warranting careful consideration of dosage in therapeutic applications. Behavioural responses have been validated as a marker of an organism's motor neuron functioning (Zhu and Goodhill 2023). The zebrafish larvae will exhibit a variety of simple and complicated behavioural patterns, and cognitive actions when exposed to various stimuli (Nishimura et al. 2015). The larvae above 40 μ M concentration of artemisinin failed to travel all the regions of the ice tray when compared to larvae in the control. Furthermore,

behavioural analysis of zebrafish larvae exposed to 160 μM artemisinin revealed abnormal behaviour characterized by reduced movements. Similar aberrant behavioural patterns were observed in larvae exposed to acrylamide, a neurotoxin known to disrupt neural communication and induce neural plasticity abnormalities (Krishnan and Kang 2019). On the other hand, the larvae treated with lower concentrations of artemisinin (10, 20, and 40 μM) explored the entire ice tray, much like the control group larvae. Notably, the VC group larvae travelled similarly to the control, which indicates that 0.1% DMSO did not induce any cognitive impairment in the larvae. Since artemisinin can cross the BBB and the brain is susceptible to oxidative stress and neuronal damage, these behavioural assessments back our hypothesis of utilising artemisinin as a therapeutic drug to treat oxidative stress. We further examined the impact of artemisinin in zebrafish larvae exposed to H_2O_2 -induced oxidative stress by quantifying the expression of essential antidiabetic and antioxidant genes in this study. The investigation into the gene expression revealed valuable insights into the molecular mechanism that governs the antidiabetic and antioxidant properties of artemisinin. We observed a significant ($p < 0.05$) downregulation in the expression of PI3K, AKT, NRF2, and CAT genes in the H_2O_2 -treated group at 96 hpf. However, after treatment with artemisinin, all the genes have been upregulated severalfold in the stress-induced zebrafish larvae. The findings of our study corroborate prior research suggesting plant bioactive compounds can effectively enhance the expression of genes responsible for the downstream activation of the PI3K/AKT signalling pathway (Muthusamy et al. 2008). This supports our claim that artemisinin can be used as a therapeutic intervention for diabetes and oxidative stress by targeting the PI3K/AKT signalling pathway.

Studies showed that decreased insulin sensitivity leads to hyperglycaemia and disrupts the equilibrium between the oxidants and antioxidants within the body (Eguchi et al. 2021). It was reported that reduced insulin sensitivity provokes the ROS and contributes to the development of insulin resistance (Salazar-García and Corona 2021). The PI3K/AKT pathway is crucial to these activities since it regulates the uptake of glucose while also maintaining the redox equilibrium (Verma et al. 2023). When insulin sensitivity is reduced, dysregulation of the PI3K/AKT pathway occurs and interferes with its capability to efficiently enable glucose transport and maintain a balanced redox environment. As a result, increased ROS generation raises insulin resistance, establishing a vicious cycle in which reduced insulin sensitivity promotes oxidative stress, worsening insulin signalling and sustaining metabolic dysfunction. Our research findings indicated that artemisinin activated the PI3K/AKT signalling cascade by binding to their catalytic sites. For instance, phosphorylation of AKT leads to the inhibition of AS160

and GSK-3 β (Yoeli-Lerner et al. 2009). The inhibition of AS160 by AKT phosphorylation results in the translocation of GLUT4 vesicles, which allows the passage of glucose molecules from the blood to the cytoplasm (Sharma and Dey 2021). Activated GSK-3 β was reported to regulate the storage of glucose by inhibiting glycogen synthase and the expression of antioxidant-responsive elements (ARE) by NRF2 ubiquitination (Chen et al. 2016). However, AKT activation by artemisinin will inhibit the GSK-3 β , and result in glycogen storage and ARE expression to combat hyperglycaemia and oxidative stress (Fig. 11).

Briefly, we have evaluated the anti-diabetic and anti-oxidant potential of artemisinin through the PI3K/AKT signalling pathway using molecular docking and in vitro analysis. Our in silico anti-diabetic analysis highlighted that artemisinin has the potential to bind with AKT, as a result further significant activation of downstream proteins can happen and may lead to glucose transporter type 4 (GLUT4) and NRF2 translocation for the transport of glucose and glycogen synthesis, and ARE expression, respectively. On the other hand, the high binding affinity with the anti-oxidant enzyme CAT highlights the importance of artemisinin in reducing the H_2O_2 free radicals, generated as a by-product of energy metabolism to protect the body from cell death and tissue damage. Furthermore, the in vitro analysis of the artemisinin showed significant anti-diabetic and anti-oxidant properties as well. The zebrafish embryo–larvae developmental toxicity analysis showed notable results to consider artemisinin as non-toxic. Further analysis of the zebrafish larvae behavioural pattern proved that artemisinin can be used as a therapeutic intervention for treating diabetics and oxidative stress. Further studies using higher experimental models will be needed to understand the complete molecular mechanism of artemisinin in regulating insulin sensitivity through the PI3K/AKT signalling pathway.

Conclusion

Our study can be a potential breakthrough towards the anti-diabetic and anti-oxidant properties of artemisinin. The results of our in silico studies highlighted the potential of artemisinin's mechanism of action via the PI3K/AKT signalling pathway. We also noted promising outcomes in the in vitro analysis while evaluating both anti-diabetic and anti-oxidant properties of artemisinin. The developmental and behavioural toxicity analysis did not exhibit any harmful repercussions, proving that artemisinin can be used as a therapeutic drug against diabetics and oxidative stress. Furthermore, the gene expression studies confirmed the plausible mechanism of artemisinin in regulating hyperglycaemia and oxidative stress. Hence, we conclude

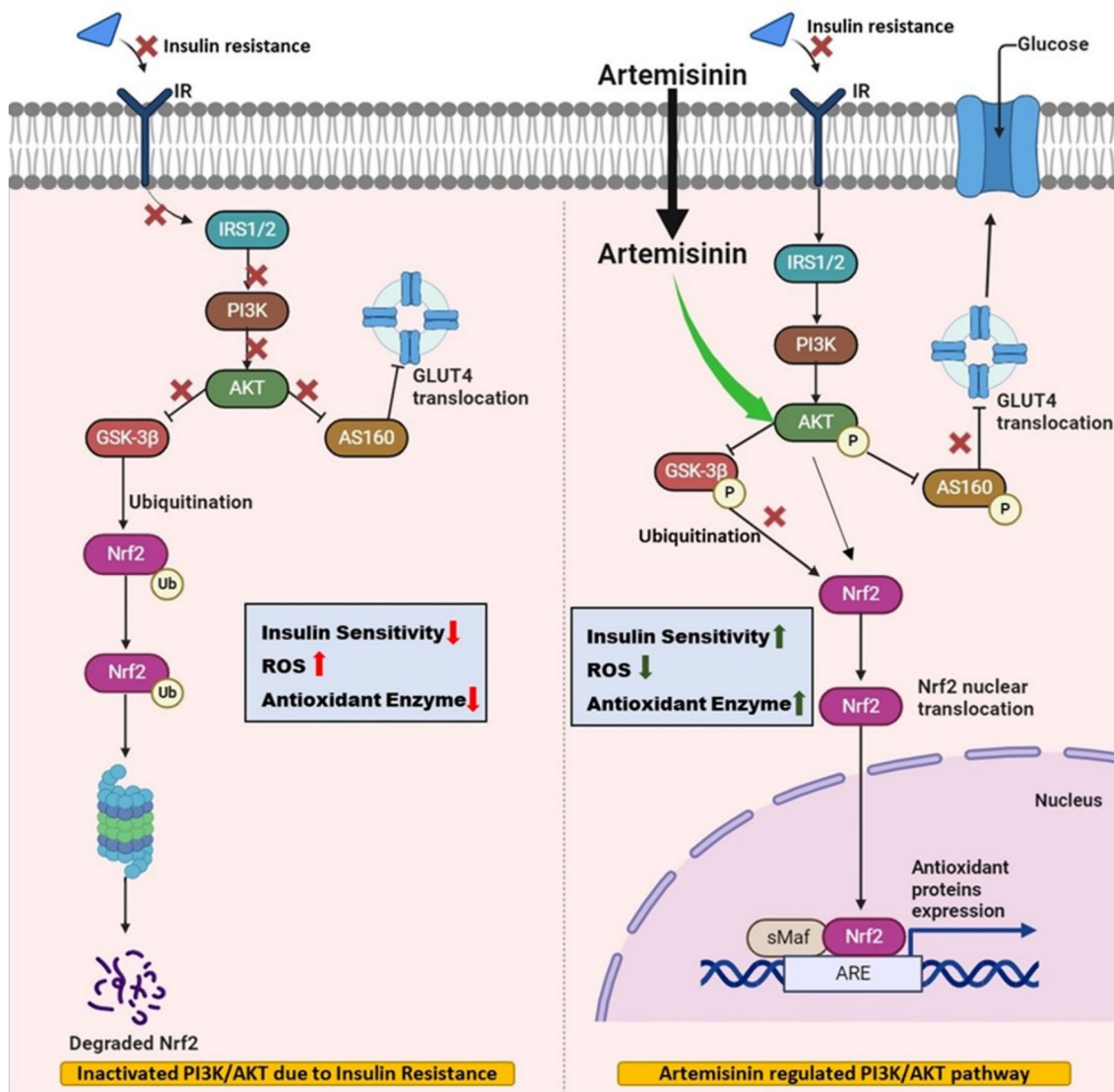


Fig. 11 The figure illustrates the hypothesized mechanism by which artemisinin regulates the PI3K/AKT signalling pathway to mitigate insulin sensitivity and oxidative stress. Artemisinin’s interactions

with key proteins in the pathway are depicted, highlighting its potential therapeutic role in managing metabolic disorders characterized by insulin resistance and oxidative damage

that artemisinin can be taken for further studies in higher experimental models to develop an efficient dual intervention for insulin sensitivity and oxidative stress.

Supplementary Information The online version contains supplementary material available at <https://doi.org/10.1007/s13205-024-04050-2>.

Acknowledgements The authors would like to acknowledge the funding support by the Researchers Supporting Project number (RSP2024R371), King Saud University, Riyadh, Saudi Arabia. The authors also thankful to the Saveetha School of Engineering, Saveetha Institute of Medical and Technical Sciences, India for their essential support in facilitating the successful completion of work conducted at the Zebra Fish Laboratory, Drug Testing Laboratory, and for their equipment such as fluorescent microscope and ELISA reader.

Data availability The data are available from the corresponding author upon reasonable request.

Declarations

Conflict of interest The authors declare that they have no conflict of interest.

Ethical approval No ethical approval was required for the current study as it did not deal with any human or animal samples.

Consent to participate Not applicable.

Consent to publish Not applicable.

References

- Alam MN, Bristi NJ, Rafiquzzaman M (2013) Review on in vivo and in vitro methods evaluation of antioxidant activity. *Saudi Pharm J* 21:143–152. <https://doi.org/10.1016/j.jsps.2012.05.002>
- Anza M, Endale M, Cardona L et al (2021) Antimicrobial activity, in silico molecular docking, ADMET and DFT analysis of secondary metabolites from roots of three Ethiopian medicinal plants. *Adv Appl Bioinform Chem* 14:117–132. <https://doi.org/10.2147/AABC.S323657>
- Asmat U, Abad K, Ismail K (2016) Diabetes mellitus and oxidative stress—A concise review. *Saudi Pharm J* 24:547–553. <https://doi.org/10.1016/j.jsps.2015.03.013>
- Balakrishnan D, Pragathiswaran C, Thanikasalam K, et al (2022) Molecular Docking and In Vitro Inhibitory Effect of Polyaniline (PANI)/ZnO Nanocomposite on the Growth of Struvite Crystal: a Step Towards Control of UTI. *Appl Biochem Biotechnol* 194:4462–4476. <https://doi.org/10.1007/s12010-022-03911-x>
- Balamurugan V, Ragavendran C, Arulbalachandran D, et al (2024) Green synthesis of silver nanoparticles using *Pandanus tectorius* aerial root extract: Characterization, antibacterial, cytotoxic, and photocatalytic properties, and ecotoxicological assessment. *Inorg Chem Commun* 168:112882. <https://doi.org/10.1016/j.inoche.2024.112882>
- Camaya I, Donnelly S, O'Brien B (2022) Targeting the PI3K/Akt signaling pathway in pancreatic β -cells to enhance their survival and function: an emerging therapeutic strategy for type 1 diabetes. *J Diabetes* 14:247–260. <https://doi.org/10.1111/1753-0407.13252>
- Chen X, Liu Y, Zhu J et al (2016) GSK-3 β downregulates Nrf2 in cultured cortical neurons and in a rat model of cerebral ischemia-reperfusion. *Sci Rep* 6:20196. <https://doi.org/10.1038/srep20196>
- Dambal VY, Selvan KP, Lite C et al (2017) Developmental toxicity and induction of vitellogenin in embryo-larval stages of zebrafish (*Danio rerio*) exposed to methyl paraben. *Ecotoxicol Environ Saf* 141:113–118. <https://doi.org/10.1016/j.ecoenv.2017.02.048>
- Dej-adisai S, Rais IR, Wattanapromsakul C, Pitakbut T (2021) Alpha-glucosidase inhibitory assay-screened isolation and molecular docking model from *Bauhinia pulla* active compounds. *Molecules* 26:5970. <https://doi.org/10.3390/molecules26195970>
- Echeazarra L, Hortigón-Vinagre MP, Casis O, Gallego M (2021) Adult and Developing Zebrafish as Suitable Models for Cardiac Electrophysiology and Pathology in Research and Industry. *Front Physiol* 11:1. <https://doi.org/10.3389/fphys.2020.607860>
- Eguchi N, Vaziri ND, Dafae DC, Ichii H (2021) The role of oxidative stress in pancreatic β cell dysfunction in diabetes. *Int J Mol Sci* 22:1509. <https://doi.org/10.3390/ijms22041509>
- Ekambaram R, Sugumar M, Swaminathan E et al (2021) Design and fabrication of electrospun *Morinda citrifolia*-based nanofibrous scaffold as skin wound dressing material: in vitro and in silico analysis. *Biomed Mater* 16:045014. <https://doi.org/10.1088/1748-605X/abef59>
- El-Askary H, Salem HH, Abdel Motal A (2022) Potential mechanisms involved in the protective effect of Dicafeoylquinic acids from *Artemisia annua* L. Leaves against diabetes and its complications. *Molecules* 27:857. <https://doi.org/10.3390/molecules27030857>
- Ghanbari M, Sadeghimahalli F (2022) Aqueous and alcoholic extracts of *Artemisia annua* L. improved insulin resistance via decreasing TNF- α , IL-6 and free fatty acids in high-fat diet/streptozotocin-induced diabetic mice. *Avicenna J Phytomed.* <https://doi.org/10.22038/AJP.2021.18829>
- Ghanbari M, Shokrzadeh Lamuki M, Sadeghimahalli F et al (2023) Oxidative stress in liver of streptozotocin-induced diabetic mice fed a high-fat diet: a treatment role of *Artemisia annua* L. *Endocr Regul* 57:242–251. <https://doi.org/10.2478/enr-2023-0027>
- Hu Y, Yang L, Lu Y et al (2022) Systems network pharmacology-based prediction and analysis of potential targets and pharmacological mechanism of *Actinidia chinensis* planch. Root extract for application in hepatocellular carcinoma. *Evid Based Complement Altern Med* 2022:1–17. <https://doi.org/10.1155/2022/2116006>
- Hullatti K, Telagari M (2015) In-vitro α -amylase and α -glucosidase inhibitory activity of *Adiantum caudatum* Linn. and *Celosia argentea* Linn. extracts and fractions. *Indian J Pharmacol* 47:425. <https://doi.org/10.4103/0253-7613.161270>
- Issac PK, Guru A, Chandrakumar SS et al (2020) Molecular process of glucose uptake and glycogen storage due to hamamelitannin via insulin signalling cascade in glucose metabolism. *Mol Biol Rep* 47:6727–6740. <https://doi.org/10.1007/s11033-020-05728-5>
- Kamaraj N, Velumani K, Guru A, Issac PK (2023) Antihyperglycemic activity of 14-deoxy, 11, 12-didehydro andrographolide on streptozotocin-nicotinamide induced type 2 diabetic rats. *Mol Biol Rep* 50:9875–9886. <https://doi.org/10.1007/s11033-023-08878-4>
- Klayman DL (1985) Qinghaosu (artemisinin): an antimalarial drug from China. *Science* 228:1049–1055. <https://doi.org/10.1126/science.3887571>
- Kotha RR, Tareq FS, Yildiz E, Luthria DL (2022) Oxidative stress and antioxidants—a critical review on in vitro antioxidant assays. *Antioxidants* 11:2388. <https://doi.org/10.3390/antiox11122388>
- Krishnan M, Kang SC (2019) Vitexin inhibits acrylamide-induced neuroinflammation and improves behavioral changes in zebrafish larvae. *Neurotoxicol Teratol* 74:106811. <https://doi.org/10.1016/j.ntt.2019.106811>
- Lalhmingshui K, Jagetia GC (2018) Evaluation of the free-radical scavenging and antioxidant activities of Chilauni Schima Wallichii Korth in vitro. *Futur Sci OA.* <https://doi.org/10.4155/fsoa-2017-0086>
- Le D, Han S, Ahn J et al (2022) Analysis of antioxidant phytochemicals and anti-inflammatory effect from *Vitex rotundifolia* L.f. *Antioxidants* 11:454. <https://doi.org/10.3390/antiox11030454>
- Lennicke C, Cochemé HM (2021) Redox metabolism: ROS as specific molecular regulators of cell signaling and function. *Mol Cell* 81:3691–3707. <https://doi.org/10.1016/j.molcel.2021.08.018>
- Muthusamy VS, Anand S, Sangeetha KN et al (2008) Tannins present in *Cichorium intybus* enhance glucose uptake and inhibit adipogenesis in 3T3-L1 adipocytes through PTP1B inhibition. *Chem Biol Interact* 174:69–78. <https://doi.org/10.1016/j.cbi.2008.04.016>
- Nakamura H, Takada K (2021) Reactive oxygen species in cancer: current findings and future directions. *Cancer Sci* 112:3945–3952. <https://doi.org/10.1111/cas.15068>
- Neagu E, Paun G, Albu C et al (2023) *Artemisia abrotanum* and *Symphytum officinale* polyphenolic compounds-rich extracts with potential application in diabetes management. *Metabolites* 13:354. <https://doi.org/10.3390/metabo13030354>
- Nisa FY, Rahman MA, Saha S et al (2023) Unraveling *Tamarindus indica* pulp-derived green magnesium oxide nanoparticles for cardioprotective potential against doxorubicin-induced cardiomyopathy: a comprehensive biochemical and gene expression study. *ACS Omega* 8:45626–45644. <https://doi.org/10.1021/acsomega.3c05851>
- Nishimura Y, Murakami S, Ashikawa Y et al (2015) Zebrafish as a systems toxicology model for developmental neurotoxicity testing. *Congenit Anom (kyoto)* 55:1–16. <https://doi.org/10.1111/cga.12079>
- Pedersen-Bjergaard U, Thorsteinsson B (2017) Reporting severe hypoglycemia in type 1 diabetes: facts and pitfalls. *Curr Diab Rep* 17:1–11. <https://doi.org/10.1007/S11892-017-0965-1/METRICS>
- Pereira AG, Fraga-Corral M, Silva A et al (2024) Unraveling the bioactive potential of *Camellia japonica* edible flowers: profiling antioxidant substances and in vitro bioactivity assessment. *Pharmaceuticals* 17:946. <https://doi.org/10.3390/ph17070946>

- Phoswa WN, Khaliq OP (2021) The role of oxidative stress in hypertensive disorders of pregnancy (preeclampsia, gestational hypertension) and metabolic disorder of pregnancy (gestational diabetes mellitus). *Oxid Med Cell Longev* 2021:1–10. <https://doi.org/10.1155/2021/5581570>
- Pizzino G, Irrera N, Cucinotta M et al (2017) Oxidative stress: harms and benefits for human health. *Oxid Med Cell Longev* 2017:1–13. <https://doi.org/10.1155/2017/8416763>
- Salazar-García M, Corona JC (2021) The use of natural compounds as a strategy to counteract oxidative stress in animal models of diabetes mellitus. *Int J Mol Sci* 22:7009. <https://doi.org/10.3390/ijms22137009>
- Sant KE, Timme-Laragy AR (2018) Zebrafish as a model for toxicological perturbation of yolk and nutrition in the early embryo. *Curr Environ Heal Reports* 5:125–133. <https://doi.org/10.1007/s40572-018-0183-2>
- Sathish Kumar P, Kannan ND (2021) A system-level approach to investigate alloxan-induced toxicity in microtubule-binding protein to lead type 2 diabetes mellitus. *Mol Divers* 25:911–924. <https://doi.org/10.1007/s11030-020-10075-5>
- Sharafati-Chaleshtori R, Nickdasti A, Mortezaipoor E et al (2021) Artemisia species as a new candidate for diabetes therapy: a comprehensive review. *Curr Mol Med* 21:832–849. <https://doi.org/10.2174/1566524020999210101234317>
- Sharma M, Dey CS (2021) AKT ISOFORMS-AS160-GLUT4: The defining axis of insulin resistance. *Rev Endocr Metab Disord* 22:973–986. <https://doi.org/10.1007/s11154-021-09652-2>
- Shori AB (2015) Screening of antidiabetic and antioxidant activities of medicinal plants. *J Integr Med* 13:297–305. [https://doi.org/10.1016/S2095-4964\(15\)60193-5](https://doi.org/10.1016/S2095-4964(15)60193-5)
- Singh AK, Rana HK, Singh V et al (2021) Evaluation of antidiabetic activity of dietary phenolic compound chlorogenic acid in streptozotocin induced diabetic rats: molecular docking, molecular dynamics, in silico toxicity, in vitro and in vivo studies. *Comput Biol Med* 134:104462. <https://doi.org/10.1016/j.combiomed.2021.104462>
- Singh A, Kukreti R, Saso L, Kukreti S (2022) Mechanistic insight into oxidative stress-triggered signaling pathways and type 2 diabetes. *Molecules* 27:950. <https://doi.org/10.3390/molecules27030950>
- Su X-Z, Miller LH (2015) The discovery of artemisinin and the nobel prize in physiology or medicine. *Sci China Life Sci* 58:1175–1179. <https://doi.org/10.1007/s11427-015-4948-7>
- Sudhakaran G, Rajesh R, Almutairi BO et al (2023) Nimbin analogs stimulate glucose uptake and glycogen storage in the insulin signalling cascade by enhancing the IRTK, PI3K and Glut-4 mechanism in myotubes. *Tissue Cell* 82:102104. <https://doi.org/10.1016/j.tice.2023.102104>
- Surya M, Sampath S, Vairamuthu SB, et al (2024) Aloe vera - mediated silver-selenium doped fucoidan nanocomposites synthesis and their multi-faceted biological evaluation of antimicrobial, antioxidant and cytotoxicity activity. *Mater Technol* 39. <https://doi.org/10.1080/10667857.2024.2331899>
- Teo ZL, Tham Y-C, Yu M et al (2021) Global prevalence of diabetic retinopathy and projection of burden through 2045. *Ophthalmology* 128:1580–1591. <https://doi.org/10.1016/j.ophtha.2021.04.027>
- Theivendran S, Gu Z, Tang J et al (2022) Nanostructured organosilica nitric oxide donors intrinsically regulate macrophage polarization with antitumor effect. *ACS Nano* 16:10943–10957. <https://doi.org/10.1021/acsnano.2c03348>
- Verma K, Jaiswal R, Paliwal S et al (2023) An insight into PI3k/Akt pathway and associated protein–protein interactions in metabolic syndrome: a recent update. *J Cell Biochem* 124:923–942. <https://doi.org/10.1002/jcb.30433>
- Yao Q, Zou X, Liu S et al (2022) Oxidative stress as a contributor to insulin resistance in the skeletal muscles of mice with Polycystic Ovary syndrome. *Int J Mol Sci* 23:11384. <https://doi.org/10.3390/ijms231911384>
- Yedjou CG, Grigsby J, Mbemi A et al (2023) The management of diabetes mellitus using medicinal plants and vitamins. *Int J Mol Sci* 24:9085. <https://doi.org/10.3390/ijms24109085>
- Yoeli-Lerner M, Chin YR, Hansen CK, Toker A (2009) Akt/protein kinase B and glycogen synthase kinase-3 β signaling pathway regulates cell migration through the NFAT1 transcription factor. *Mol Cancer Res* 7:425–432. <https://doi.org/10.1158/1541-7786.MCR-08-0342>
- Zampini IC, Ordoñez RM, Isla MI (2010) Autographic assay for the rapid detection of antioxidant capacity of liquid and semi-solid pharmaceutical formulations using ABTS \bullet + immobilized by gel entrapment. *AAPS PharmSciTech* 11:1159–1163. <https://doi.org/10.1208/s12249-010-9484-y>
- Zhong HA, Goodwin DT (2024) Selectivity studies and free energy calculations of AKT inhibitors. *Molecules* 29:1233. <https://doi.org/10.3390/molecules29061233>
- Zhu SI, Goodhill GJ (2023) From perception to behavior: the neural circuits underlying prey hunting in larval zebrafish. *Front Neural Circuits*. <https://doi.org/10.3389/fncir.2023.1087993>

Springer Nature or its licensor (e.g. a society or other partner) holds exclusive rights to this article under a publishing agreement with the author(s) or other rightsholder(s); author self-archiving of the accepted manuscript version of this article is solely governed by the terms of such publishing agreement and applicable law.